Journal of
Translational Medicine

NL101 synergizes with the BCL-2 inhibitor venetoclax through PI3K-dependent suppression of c-Myc in acute myeloid leukaemia

Ying Lu[1,3], Xia Jiang[1,2,3], Youhong Li[1,2,3], Fenglin Li[1,3], Mengting Zhao[2], Ye Lin[2], Lili Jin[1,2,3], Haihui Zhuang[1,3], Shuangyue Li[1,3], Peipei Ye[1,3], Renzhi Pei[1,3], Jie Jin[4] and Lei Jiang[1,2*]

Abstract

Background Acute myeloid leukaemia (AML) comprises a group of heterogeneous and aggressive haematological malignancies with unsatisfactory prognoses and limited treatment options. Treatments targeting B-cell lymphoma-2 (BCL-2) with venetoclax have been approved for patients with AML, and venetoclax-based drug combinations are becoming the standard of care for older patients unfit for intensive chemotherapy. However, the therapeutic duration of either single or combination strategies is limited, and the development of resistance seems inevitable. Therefore, more effective combination regimens are urgently needed.

Methods The efficacy of combination therapy with NL101, a SAHA-bendamustine hybrid, and venetoclax was evaluated in preclinical models of AML including established cell lines, primary blasts from patients, and animal models. RNA-sequencing and immunoblotting were used to explore the underlying mechanism.

Results NL101 significantly potentiated the activity of venetoclax in AML cell lines, as evidenced by the enhanced decrease in viability and induction of apoptosis. Mechanistically, the addition of NL101 to venetoclax decreased the stability of the antiapoptotic protein myeloid cell leukaemia-1 (MCL-1) by inhibiting ERK, thereby facilitating the release of BIM and triggering mitochondrial apoptosis. Moreover, the strong synergy between NL101 and venetoclax also relied on the downregulation of c-Myc via PI3K/Akt/GSK3β signalling. The combination of NL101 and venetoclax synergistically eliminated primary blasts from 10 AML patients and reduced the leukaemia burden in an MV4-11 cell-derived xenograft model.

Conclusions Our results encourage the pursuit of clinical trials of combined treatment with NL101 and venetoclax and provide a novel venetoclax-incorporating therapeutic strategy for AML.

Keywords AML, NL101, Venetoclax, Apoptosis, MCL-1, c-Myc

*Correspondence:
Lei Jiang
jianglei@nbu.edu.cn
Full list of author information is available at the end of the article

Lu *et al. Journal of Translational Medicine*　　(2024) 22:867

Page 2 of 18

Background

Acute myeloid leukaemia (AML), the most common type of leukaemia in adults, is a heterogeneous malignancy characterized by uncontrolled clonal expansion and differentiation arrest of immature haematopoietic blast cells. Although most AML patients achieve initial remission after standard induction chemotherapy, known as the "3+7" (3 days of daunorubicin+7 days of cytarabine) regimen, many patients experience disease relapse and have a dismal prognosis, with 5-year survival rates of at most 40% in younger patients (aged<60 years) and less than 15% in older patients (aged≥60 years) [1, 2]. Given the median age at diagnosis of 68 years [3], this unfit population represents the majority of AML patients, in whom the disease is generally incurable, emphasizing the unmet need for more effective but less intensive therapeutic approaches.

The clarification of the molecular pathogenesis of AML has spurred the approval of numerous novel targeted agents for different AML indications since 2017, for example, the fms-like tyrosine kinase 3 (FLT3) inhibitors midostaurin and gilteritinib, the isocitrate dehydrogenase (IDH) inhibitors ivosidenib and enasidenib, the B-cell lymphoma-2 (BCL-2) inhibitor venetoclax, the anti-CD33 monoclonal antibody gemtuzumab ozogamicin, CPX-351, and oral azacitidine, ushering in a new era of targeted therapy for AML management [4, 5]. Among these newly approved drugs, venetoclax has shown modest activity in patients with relapsed or refractory (R/R) AML when used as a single agent [6] but has increased response rates and prolonged overall survival in newly diagnosed AML patients who are ≥75 years of age or are unsuitable for intensive chemotherapy when used combined with hypomethylating agents (HMAs) or low-dose cytarabine (LDAC) [7–10]. Currently, these combinations are widely considered new standards of care for older, unfit, and treatment-naive patients with AML, and more venetoclax-based combination regimens are being focused on in both preclinical and clinical studies of AML.

Dysregulation of histone deacetylases (HDACs) frequently occurs in AML [11], supporting the rationale for the development of HDAC inhibitors (HDACi) as new antileukaemic options. Although vorinostat (suberoylanilide hydroxamic acid, SAHA) monotherapy does not show sufficient activity in relapsed or treatment-naive AML patients [12], cooperative effects are observed in multiple myeloma (MM) cells treated with entinostat in combination with bendamustine, an alkylator with DNA-damaging properties [13]. Therefore, a SAHA-bendamustine hybrid, NL101 (also known as EDO-S101), is designed by replacement of the butyric acid of bendamustine with the hydroxamic acid of SAHA, preserving the positive qualities of both drugs [14]. NL101 exhibits considerable toxicity against MM and B-cell lymphoma cells [15, 16], highlighting its potential in treating haematologic malignancies. In addition, compared with single bendamustine or SAHA, NL101 exhibits superior anti-AML activity both in vitro and in vivo [14]. Moreover, NL101 exhibits strong synergy with cytarabine, daunorubicin, the PARP inhibitor BMN673, and the proteasome inhibitors bortezomib and carfilzomib [17–20]. These encouraging results prompt us to investigate whether NL101 is capable of increasing sensitivity to venetoclax in preclinical models of AML.

In the present study, we aim to determine the therapeutic efficacy of NL101 combined with venetoclax in preclinical models of AML including established cell lines in vitro, primary blasts from AML patients ex vivo, and an MV4-11 cell-derived animal model in vivo. Molecular mechanisms responsible for the synergy between NL101 and venetoclax are also investigated. Therefore, our data provide a strong rationale for using this combination regimen as a potential therapeutic strategy for AML patients.

Methods

Reagents

NL101 was provided by Minsheng Institute of Pharmaceutical Research (Hangzhou, China) [14]. Venetoclax was purchased from Selleck Chemicals (#S8048; Houston, TX, USA). MG-132 (#HY-13259), Lys05 (#HY-12855A), MK2206 (#HY-108232), AR-A014418 (#HY-10512), and vorinostat (#HY-10221) were purchased from MedChemExpress (MCE; NJ, USA). The anti-human CD45 antibody was purchased from Multisciences Biotech (#F11045A02; Hangzhou, China).

Cell lines

The human AML cell lines MV4-11 and THP-1 were purchased from the American Type Culture Collection (ATCC; Manassas, VA, USA), and the MOLM-13 cell line was purchased from the Deutsche Sammlung von Mikroorganismen und Zellkulturen (DSMZ; Braunschweig, Germany). The cells were cultured in Roswell Park Memorial Institute (RPMI)-1640 medium (HyClone, UT, USA) supplemented with 10% foetal bovine serum (FBS; AusgeneX, Molendinar, QLD, Australia), 100 U/mL penicillin/streptomycin (Solarbio, Beijing, China), and 2 mM L-glutamine (Solarbio) and were maintained at 37 °C in a humidified chamber containing 5% CO_2. Each cell line was authenticated by short tandem repeat profiling and tested negative for mycoplasma contamination. For the in vitro experiments, cells with fewer than 15 passages were used.

Lu *et al. Journal of Translational Medicine*   (2024) 22:867

Page 3 of 18

Patient specimens

AML patients who met the MICM (morphology, immunology, cytogenetic and molecular biology) diagnosis and FAB/WHO classification standards with complete clinical information were included, and those with other malignant diseases were excluded in this study. Bone marrow or peripheral blood samples were collected from AML patients under a protocol approved by the Human Ethics Committee of the Affiliated People's Hospital of Ningbo University after written informed consent was obtained from each patient in accordance with the Declaration of Helsinki. Primary AML cells were isolated by Ficoll-Hypaque density gradient centrifugation and grown in culture medium supplemented with 20% FBS. Cell suspensions containing more than 80% viable cells, as determined by trypan blue staining, were utilized for relevant experiments.

Cell viability

AML cell lines ($1-3\times10^4$ cells/well, depending on the cell type) or cells isolated from primary AML samples (1×10^5 cells/well) were seeded in 96-well plates in triplicate and treated with the indicated doses of venetoclax and NL101 alone or in combination. Cell viability was subsequently determined using CellTiter 96 AQueous One Solution (Promega, Madison, WI, USA) according to the manufacturer's instructions. The drug concentrations that resulted in a 50% reduction in cell viability (IC_{50}) were calculated using nonlinear regression analysis. The combination index (CI) was calculated according to the Chou-Talalay method using CompuSyn software (version 1.0) [21]. A CI of < 1 indicates synergism. Since drug combinations were non-constant in this study, a normalized isobologram was generated.

Flow cytometry

Apoptosis and mitochondrial membrane potential (MMP) were detected as previously described [22, 23]. All samples were analysed by flow cytometry (CytoFLEX S; Beckman Coulter Life Sciences, Indianapolis, IN, USA), and the data were analysed using CytExpert software (Beckman Coulter, version 2.4).

Western blot analysis

Mitochondria were isolated using a Cytoplasmic and Mitochondrial Protein Extraction Kit (#C500051; Sangon Biotech, Shanghai, China). Cell lysis, protein quantification, electrophoresis and gel-to-membrane transfer were performed essentially as previously reported [24]. The membranes were cut horizontally and probed with primary antibodies specific for the following proteins: PARP (#9532; Cell Signaling Technology, CST; Beverly, MA, USA, 1:1000); caspase 3 (#9662; CST, 1:1000); MCL-1 (#16225-1-AP; Proteintech, 1:1000); B-cell lymphoma-extra large (BCL-xL; #10783-1-AP; Proteintech, 1:2000); BIM (#2933; CST, 1:1000); BID (#2002; CST, 1:1000); Akt (#2920; CST, 1:1000); phospho-Akt (Ser473; #4060; CST, 1:1000); GSK3β (#9315; CST, 1:1000); phospho-GSK3β (Ser9; #9322; CST, 1:1000); cytochrome c (#66264-1-Ig; Proteintech, 1:2000); voltage-dependent anion channel (VDAC; #4661; CST, 1:1000); β-actin (#A3854; Sigma, 1:2000); and GAPDH (#60004-1-Ig; Proteintech, 1:10,000). After the membranes were incubated with the corresponding secondary antibody, i.e., goat anti-rabbit IRDye 680RD or goat anti-mouse IRDye 800CW (LI-COR Biosciences, Lincoln, NE, USA), signals were detected using an Odyssey infrared imaging system (LI-COR Biosciences). To analyse proteins with very similar molecular weights, the membranes were stripped using NCM Western Blot Stripping Buffer (#WB6200; NCM Biotech, Suzhou, China) according to the manufacturer's instructions and probed a second time. Densitometry measurements were carried out using Image J software.

Quantitative real-time PCR (qRT-PCR)

Total RNA was extracted using a TransZol Up Plus RNA Kit (#ER501-01-V2; TransGen Biotech, Beijing, China), and cDNA was synthesized from 1 μg of total RNA using a RevertAid First Strand cDNA Synthesis Kit (#K1622; Thermo Fisher Scientific, Shanghai, China) following protocols recommended by the manufacturers. qRT-PCR was performed on triplicate samples using SYBR Green I Master Mix (Roche Diagnostics, Mannheim, Germany) in a final reaction volume of 10 μL containing 1 μL of cDNA on a LightCycler 480 II instrument (Roche Diagnostics). The thermal cycling conditions were 95 °C for 5 min, followed by 45 cycles of denaturation at 95 °C for 10 s, annealing at 60 °C for 10 s, and extension at 72 °C for 10 s. Relative gene expression was determined by normalization to the expression of the GAPDH housekeeping gene, and the values were presented as fold changes relative to the control calculated using the $2^{-\Delta\Delta Ct}$ method. The primers used were as follows:

> c-Myc-Forward: CTCCACACATCAGCACAACTAC
> c-Myc-Reverse: CACTGTCCAACTTGACCCTC
> GAPDH-Forward: TGTAAAACGACGGCCAGT
> GAPDH-Reverse: CAGGAAACAGCTATGACC

RNA sequencing (RNA-seq)

Total cellular RNA was extracted using a TransZol Up Plus RNA Kit following the manufacturer's recommended protocol. The RNA quantity and purity were determined by a NanoDrop 2000 spectrophotometer

Lu *et al. Journal of Translational Medicine*   (2024) 22:867

Page 4 of 18

(Thermo Fisher Scientific). The RNA integrity was verified by an Agilent 2100 Bioanalyzer (Agilent Technologies, Santa Clara, CA, USA). To construct the sequencing library, a VAHTS Universal V6 RNA-seq Library Prep Kit was used according to the manufacturer's instructions. Transcriptome sequencing was conducted by OE Biotech Co., Ltd (Shanghai, China) on a NovaSeq 6000 instrument (Illumina, San Diego, CA, USA), and 150 bp paired-end reads were generated. After removing poor quality reads by processing the raw reads with Fastq, differential expression analysis was performed using DESeq2 based on a q value threshold of 0.05. Kyoto Encyclopedia of Genes and Genomes (KEGG) pathway enrichment analysis was performed with R (version 3.2.0) according to the hypergeometric distribution assumption.

Virus production and infection

The lentivirus vector (pEZ-Lv105) expressing c-Myc (#EX-Z2845-Lv105) was purchased from GeneCopoeia (Guangzhou, China). HEK 293T cells were transfected with 5 μg lentiviral expression plasmid together with 3.3 μg psPAX2 and 1.65 μg pMD2.G lentiviral packaging plasmids for 12 h. The media was replaced with fresh media and cells were cultured for a further 60 h. Viral supernatant was then collected and filtered through a 0.45 μm-diameter filter. AML cells were infected with lentiviral particles and stable clones were selected with 2 μg/mL puromycin.

Animal studies

All animal experiments were conducted in accordance with protocols approved by the Institutional Animal Care and Use Committee at Ningbo University Health Science Center. For establishment of the AML model, female NCG mice at 4–6 weeks of age (NOD/ShiLtJGpt-Prkdc^{em26Cd52}Il2rg^{em26Cd22}/Gpt; strain no. T001475; GemPharmatech, Nanjing, China) were inoculated via the tail vein with 1×10^7 luciferase-expressing MV4-11 cells (Day 0). Once leukaemia engraftment was confirmed on Day 7 via a noninvasive whole-body imaging system (IVIS Spectrum; PerkinElmer, Waltham, USA) after intraperitoneal injection of D-luciferin (150 mg/kg; PerkinElmer), the mice were divided into four groups (n=7 mice per group), and treatment was initiated. Venetoclax was administered at a dosage of 75 mg/kg daily by gavage for 14 days, and NL101 was intravenously injected at a dosage of 12 mg/kg daily for 2 days. For mice receiving the drug combination, venetoclax was administered prior to NL101. The mice were observed every day, and body weights were measured throughout the study period. To monitor the leukaemia burden and drug efficacy, bioluminescence imaging was performed at the indicated time points, and the signal intensity was analysed using Living Image® software (version 4.3.1; PerkinElmer). Upon the occurrence of lower extremity paralysis, the mice were euthanized, and leukaemia infiltration was assessed by flow cytometric quantification of the proportion of human CD45$^+$ cells in the bone marrow obtained from flushed tibias and femurs. Survival was monitored until the end of the experiment.

Statistical analysis

Data were expressed as the mean ± SEM of at least three independent experiments. Differences between groups were analysed using Student's *t* test or one-way analysis of variance (ANOVA) followed by Tukey's multiple comparison test with Prism software (GraphPad Software, Inc., San Diego, CA, USA). *P* values < 0.05 were considered to indicate statistical significance (*P < 0.05, **P < 0.01, and ***P < 0.001). Mouse survival was estimated using the Kaplan–Meier method, and comparisons of survival curves were performed with the log-rank (Mantel–Cox) test.

Results

NL101 combined with venetoclax synergistically decreases cell viability and induces apoptosis in AML cell lines in vitro

We first examined the single-agent activity of NL101 in 3 human AML cell lines, namely, MOLM-13, MV4-11 and THP-1 cells, and we generated dose–response curves and calculated the IC$_{50}$ values following 48 h of treatment. While NL101 was effective in all the tested AML cell lines, MOLM-13 and MV4-11 cells exhibited greater sensitivity than THP-1 cells did (Fig. 1A). Subsequently, we aimed to determine whether NL101 can sensitize AML cells to BCL-2 inhibition. As can be seen in MOLM-13 cells (Fig. 1B, upper left panel), venetoclax monotherapy dose-dependently reduced cell viability, and the addition of NL101 at sublethal concentrations substantially enhanced the activity of venetoclax. Most of the concentration pairs resulted in CI values of less than 1, which further verified the synergy between NL101 and venetoclax (Fig. 1B, upper right panel). Synergistic effects of NL101 with venetoclax were also observed in MV4-11 cells and even in venetoclax-resistant THP-1 cells (Fig. 1B, middle and lower panels). Combinations that represented synergism were also plotted in normalized isobologram profiles (Fig. S1). To investigate whether cell death following treatment with the combination of NL101 and venetoclax resulted from apoptosis, Annexin V/PI double staining and western blotting were carried out in selected AML cell lines with different genetic backgrounds. Compared with the control and single-agent treatments, the combination treatment conspicuously increased the proportion of Annexin V-positive cells (Fig. 1C and Fig. S2) and promoted the cleavage of

Lu *et al. Journal of Translational Medicine*   (2024) 22:867

Page 5 of 18
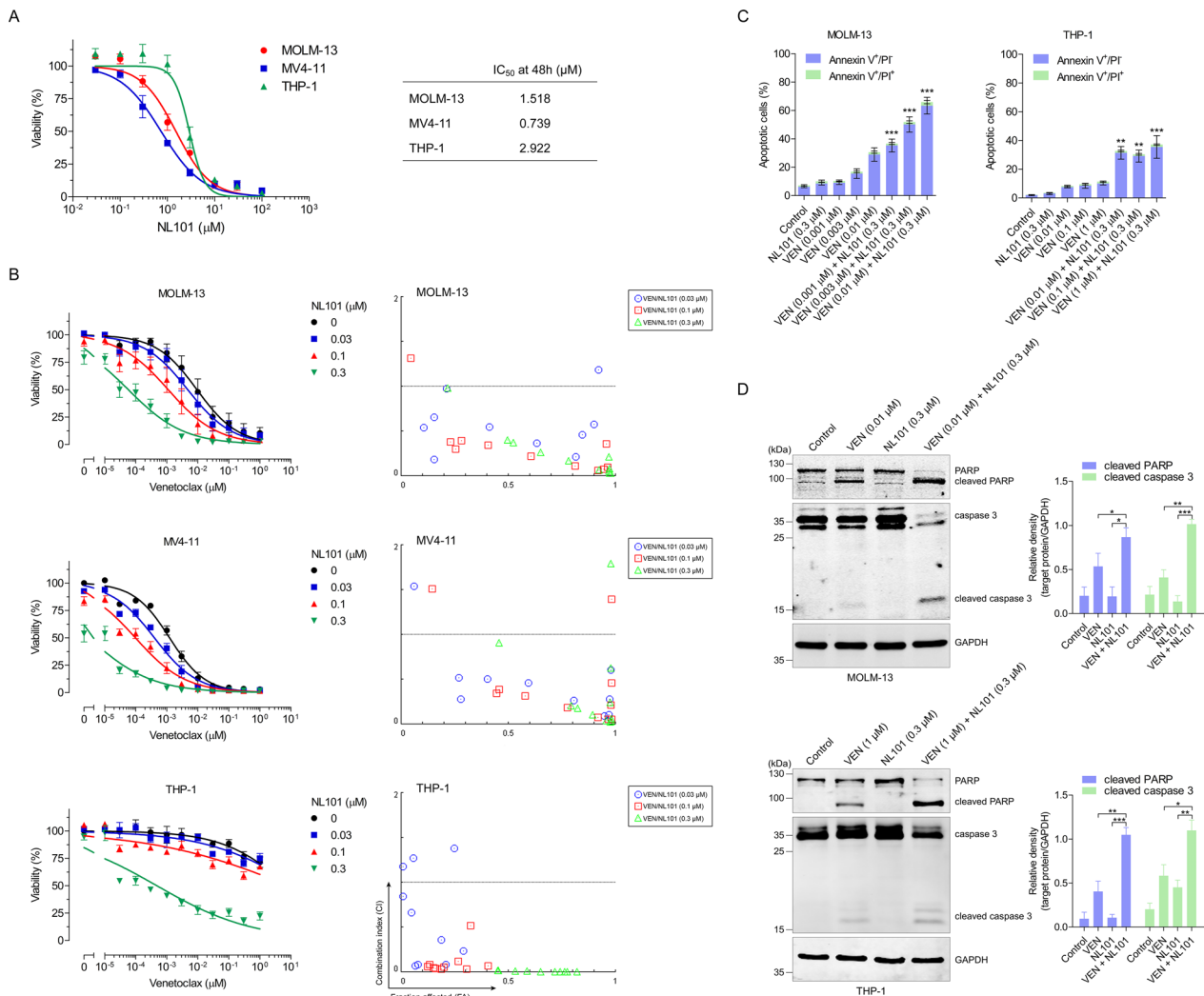
Fig. 1 NL101 in combination with venetoclax synergistically reduces cell viability and induces apoptosis. **A** Cell viability in MOLM-13, MV4-11, and THP-1 cells treated with NL101 at increasing concentrations (0.03, 0.1, 0.3, 1, 3, 10, 30, and 100 μM) for 48 h. **B** Cell viability and combination index (Fa-CI) plots in MOLM-13, MV4-11, and THP-1 cells cotreated with NL101 and venetoclax at prespecified concentrations for 48 h. **C** Flow cytometry analysis of apoptosis in MOLM-13 and THP-1 cells incubated with the indicated concentrations of NL101 and venetoclax alone or in combination for 24 h. **P < 0.01 and ***P < 0.001 versus the control group. **D** The protein levels of PARP (full-length and cleaved) and caspase 3 (full-length and cleaved) in MOLM-13 and THP-1 cells measured via western blotting. GAPDH was used as a loading control. Representative blots from three independent experiments and densitometric analyses were shown. *P < 0.05, **P < 0.01, and ***P < 0.001

caspase 3 and PARP (Fig. 1D) in both the MOLM-13 and THP-1 cells. Taken together, these results suggested that the combination of NL101 and venetoclax induced synergistic antileukaemic effects in AML cell lines in vitro.

NL101 combined with venetoclax induces mitochondrial dysfunction via ERK-dependent MCL-1 inhibition

Given the clear importance of mitochondria in apoptotic events, we assessed alterations in MMP in MOLM-13 and THP-1 cells treated with venetoclax, NL101, or their combination by staining with JC-1 dye. While the MMP was moderately affected by venetoclax monotherapy but

not by NL101 monotherapy, the combined treatment resulted in a further decline in the MMP (Fig. 2A), indicating that depolarization of the mitochondrial membrane, which is a marker of mitochondrial disruption, occurred. In line with these observations, the level of cytochrome c decreased in mitochondria and increased in the cytosol, indicating that treatment with NL101 and venetoclax resulted in the release of cytochrome c from mitochondria (Fig. 2B). The protein expression levels of members of the BCL-2 family, which are critical regulators of mitochondrial apoptosis, were subsequently measured to gain further insight into the
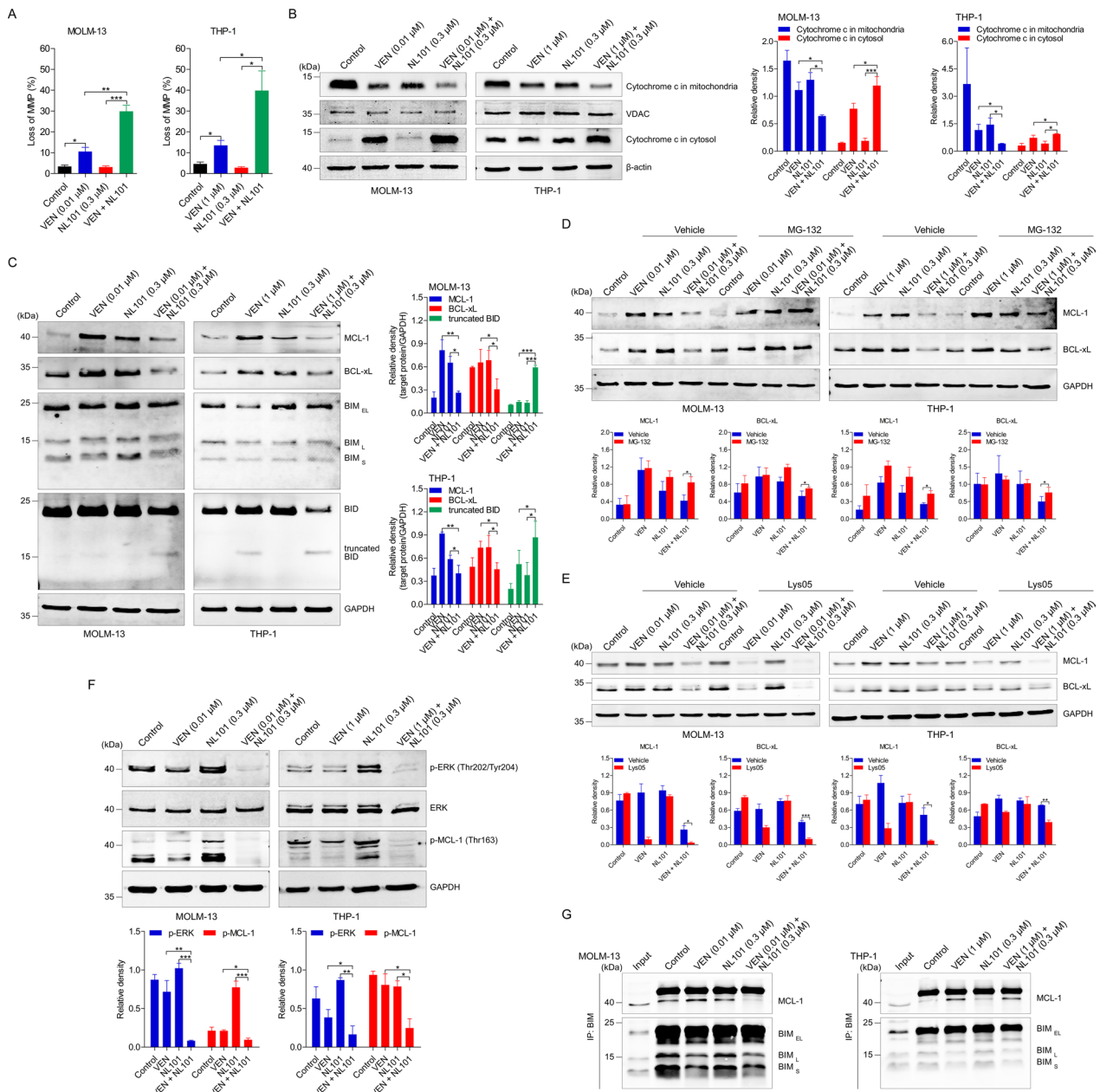
Fig. 2 NL101 combined with venetoclax promotes ERK-dependent MCL-1 inhibition. **A** The percentage of cells with MMP loss in MOLM-13 and THP-1 cells incubated with the indicated concentrations of NL101 and venetoclax alone or in combination for 24 h calculated via flow cytometry. *$P < 0.05$, **$P < 0.01$ and ***$P < 0.001$. **B** The levels of cytochrome c in the mitochondria and cytoplasm in MOLM-13 and THP-1 cells measured via western blotting. VDAC and β-actin were used as loading controls. Representative blots from three independent experiments and densitometric analyses were shown. *$P < 0.05$ and ***$P < 0.001$. **C** The levels of MCL-1, BCL-xL, BIM, and BID in MOLM-13 and THP-1 cells measured via western blotting. GAPDH was used as a loading control. Representative blots from three independent experiments and densitometric analyses were shown. *$P < 0.05$, **$P < 0.01$, and ***$P < 0.001$. **D**, **E** MOLM-13 and THP-1 cells were treated with NL101 and venetoclax alone or in combination in the absence or presence of MG-132 or Lys05. The levels of MCL-1 and BCL-xL were measured via western blotting. GAPDH was used as a loading control. Representative blots from three independent experiments and densitometric analyses were shown. *$P < 0.05$, **$P < 0.01$, and ***$P < 0.001$. **F** The levels of phosphorylated ERK and MCL-1 in MOLM-13 and THP-1 cells measured via western blotting. GAPDH was used as a loading control. Representative blots from three independent experiments and densitometric analyses were shown. *$P < 0.05$, **$P < 0.01$, and ***$P < 0.001$. **G** MOLM-13 and THP-1 cells were incubated with the indicated concentrations of NL101 and venetoclax alone or in combination for 24 h. BIM was immunoprecipitated from whole-cell lysates and the level of MCL-1 was subsequently measured. Representative blots were obtained from three independent experiments

Lu *et al. Journal of Translational Medicine*   (2024) 22:867

Page 7 of 18

associated mechanism responsible for the active interaction between venetoclax and NL101. We found that exposure of MOLM-13 and THP-1 cells to venetoclax triggered an increase in MCL-1 expression, which was sharply reduced after the addition of NL101, even though NL101 treatment alone also increased MCL-1 expression (Fig. 2C). Additionally, downregulation of another antiapoptotic protein, BCL-xL, and truncation of the proapoptotic BH-3 domain-only protein BID (tBID) were observed in both cell lines upon treatment with venetoclax in combination with NL101 (Fig. 2C). Neither agent alone nor the combination of the agents influenced the expression of BIM (Fig. 2C). To elucidate whether MCL-1 downregulation occurred at the transcriptional level, qRT-PCR was performed. To our surprise, the mRNA level of *MCL1* was increased after treatment with NL101 and venetoclax (data not shown). Preincubation with the proteasome inhibitor MG-132 (Fig. 2D), but not the lysosome inhibitor Lys05 (Fig. 2E), prevented the decreases in MCL-1 and BCL-xL protein levels induced by the combination treatment in MOLM-13 and THP-1 cells, implying the activity of a proteasome-dependent mechanism of protein degradation. Importantly, marked reductions in MCL-1 phosphorylation at Thr163 and ERK phosphorylation at Thr202/Tyr204 were observed upon the addition of NL101 to venetoclax, suggesting impaired ERK-regulated stabilization of MCL-1 (Fig. 2F). As a result, NL101 attenuated the venetoclax-induced promotion of BIM binding to MCL-1, enabling the release of free BIM to induce apoptosis by activating BAX/BAK (Fig. 2G). Collectively, these data demonstrated that the combination of NL101 with venetoclax induced mitochondrial dysfunction via MCL-1 degradation through ERK inactivation.
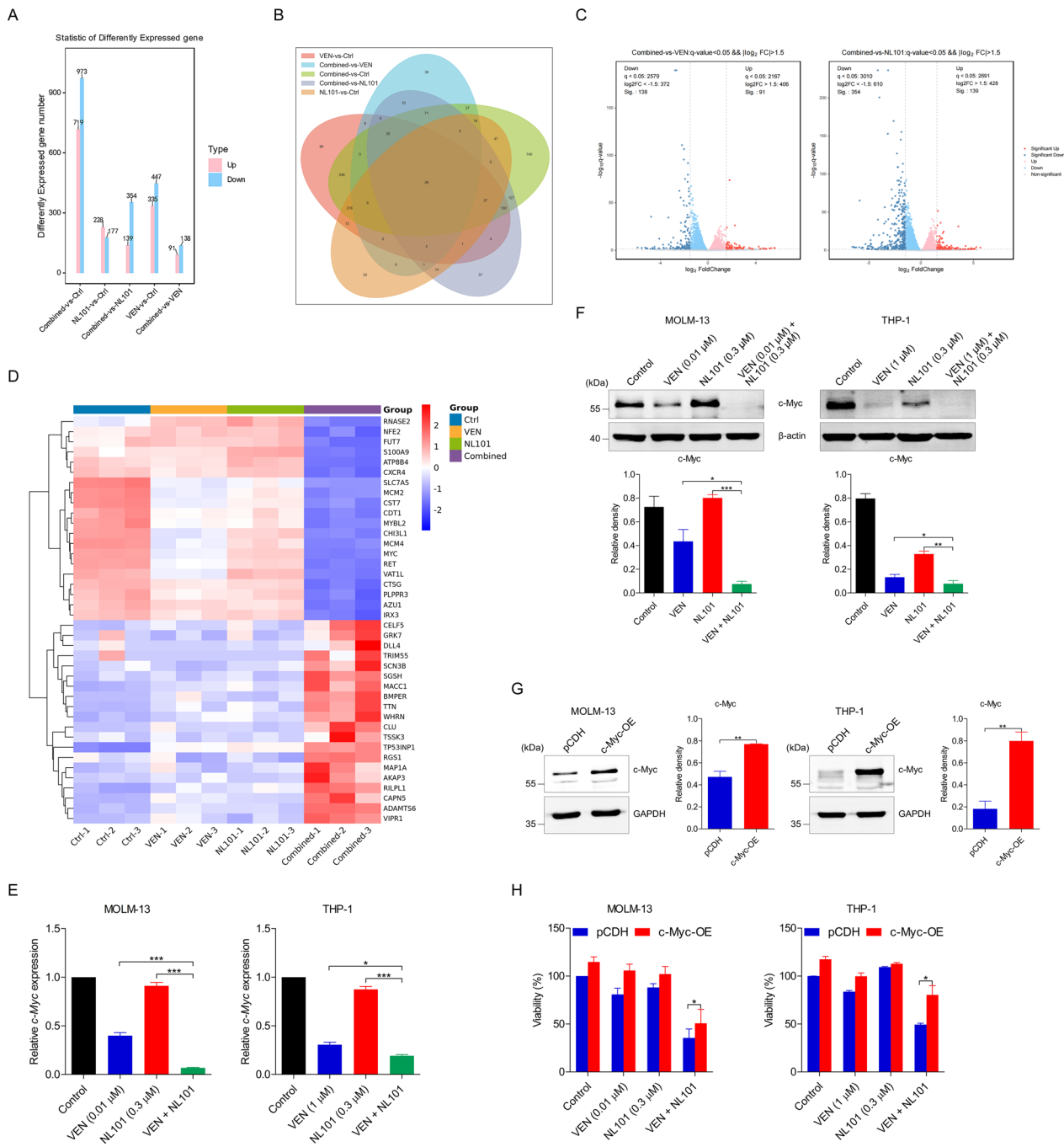
NL101 combined with venetoclax inactivates c-Myc via the PI3K/Akt/GSK3β cascade

To delineate the potential mechanism underlying the observed synergy, the transcriptomic alterations in MOLM-13 cells following treatment with venetoclax and NL101 alone or in combination were analysed via RNA-seq. The expression of 782 and 405 genes was significantly modulated relative to that in the control group by venetoclax and NL101, respectively, and 1692 genes were significantly modulated by the combination of venetoclax and NL101, indicating that the combination treatment had a greater impact on genome-wide gene regulation (Fig. 3A). The overlap of the differentially expressed genes (DEGs) in these pairwise comparisons revealed that the effect of the combined treatment with venetoclax and NL101 was not only unified but also enhanced, as evidenced by the modulation of a great number of genes that were not affected by either single treatment (Fig. 3B).

Importantly, 229 (138 downregulated and 91 upregulated) and 493 (354 downregulated and 139 upregulated) DEGs were identified between the combination treatment group and the venetoclax and NL101 single treatment groups, respectively (Fig. 3C). Among the top 20 DEGs, the most prominently affected gene was c-Myc ($\log_2$FC: ≈ -2.76; P value $= 2.92E-194$; Fig. 3D). The qRT-PCR (Fig. 3E) and western blot (Fig. 3F) data confirmed that venetoclax but not NL101 markedly reduced both the mRNA and protein levels of c-Myc in MOLM-13 and THP-1 cells, and that these levels further decreased when these two agents were combined. When the overexpression of c-Myc was induced in AML cells (Fig. 3G), the viability inhibited by the combination treatment was partially reversed (Fig. 3H), indicating the functional contribution of c-Myc to venetoclax/NL101 lethality. Next, to explore the upstream signalling cascade responsible for c-Myc downregulation, we conducted KEGG analysis. The top pathways enriched in the downregulated genes were shown in Fig. 4A, with the most prominent and relevant pathway being the PI3K/Akt signalling pathway. The phosphorylation of Akt at Ser473 and of its target GSK3β at Ser9 was suppressed in MOLM-13 and THP-1 cells in the presence of both drugs in a time-dependent manner (Fig. 4B). Moreover, pretreatment with the Akt inhibitor MK2206 or the GSK3β inhibitor AR-A014418 prevented the c-Myc-targeting effect of venetoclax combined with NL101 (Fig. 4C). Therefore, all of the above results highlighted the key role of PI3K/Akt/GSK3β-dependent inhibition of c-Myc in the synergistic interaction between venetoclax and NL101.

NL101 exhibits a cooperative effect with venetoclax superior to that of vorinostat in AML cells

Vorinostat was approved by the United States Food and Drug Administration (FDA) in 2006 for the treatment of patients with cutaneous T-cell lymphoma who had progressive, persistent, or recurrent disease or who had been treated with two systemic therapies [25, 26]. As NL101 is a derivative of vorinostat, a direct comparison between NL101 and vorinostat in terms of the venetoclax-potentiating effect was of great interest. NL101 and vorinostat exhibited comparable and nontoxic effects on MOLM-13 cells when used as single agents at a concentration of 0.1 μM, whereas they further reduced cell viability, albeit to different extents, when combined with venetoclax, with the effect of NL101 being significantly greater than that of vorinostat (Fig. 5A, left panel). Consistently, combined treatment with venetoclax and NL101 led to a greater proportion of apoptotic cells than did the combination of venetoclax and vorinostat (Fig. 5A, right panel and Fig. S3). Similar phenomena were also observed in MV4-11

Fig. 3 NL101 combined with venetoclax downregulates c-Myc. **A** The numbers of differentially expressed genes (DEGs) between the comparison groups in MOLM-13 cells by RNA sequencing. **B** Venn diagram showing the overlap of the DEGs. **C** Volcano plot of the DEGs. **D** Heatmap showing the top 20 downregulated and upregulated genes. **E** The mRNA level of *c-Myc* in MOLM-13 and THP-1 cells cotreated with venetoclax and NL101. *$P < 0.05$ and ***$P < 0.001$. **F** The protein level of c-Myc in MOLM-13 and THP-1 cells cotreated with venetoclax and NL101. β-actin was used as a loading control. Representative blots from three independent experiments and densitometric analyses were shown. *$P < 0.05$, **$P < 0.01$, and ***$P < 0.001$. **G** The protein level of c-Myc in MOLM-13 and THP-1 cells after *c-Myc* was overexpressed. GAPDH was used as a loading control. Representative blots from three independent experiments and densitometric analyses were shown. **$P < 0.01$. **H** Cell viability in MOLM-13 and THP-1 cells cotreated with venetoclax and NL101 for 24 h in the absence or presence of c-Myc overexpressoin

Lu *et al. Journal of Translational Medicine*   (2024) 22:867

Page 9 of 18
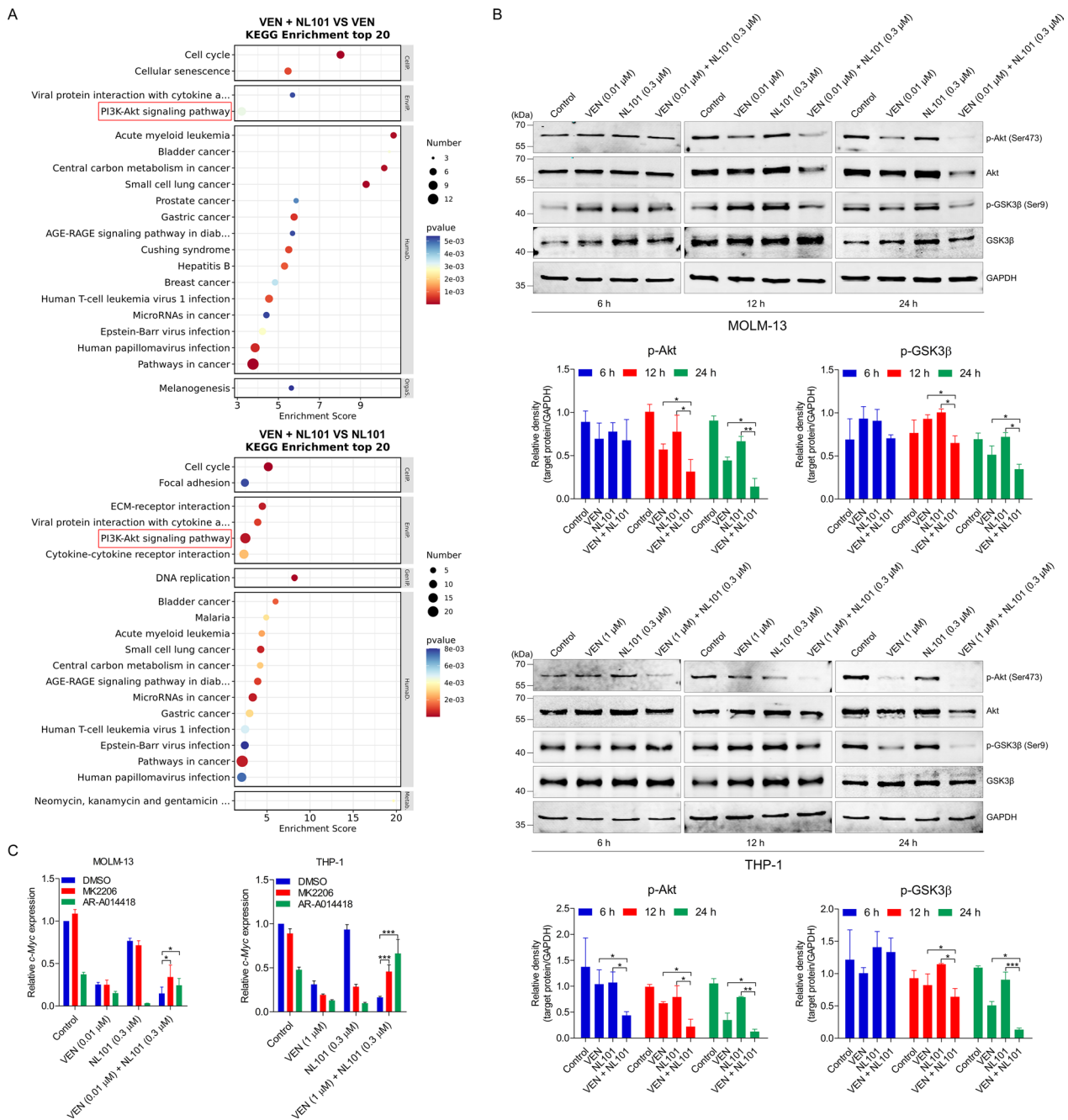
Fig. 4 NL101 combined with venetoclax inhibits the PI3K/Akt/GSK3β pathway. **A** KEGG pathway analysis of the DEGs. **B** The levels of total and phosphorylated Akt and GSK3β in MOLM-13 and THP-1 cells measured via western blotting. GAPDH was used as a loading control. Representative blots from three independent experiments and densitometric analyses were shown. *$P < 0.05$, **$P < 0.01$, and ***$P < 0.001$. **C** The mRNA level of *c-Myc* in MOLM-13 and THP-1 cells measured by qRT-PCR. *$P < 0.05$ and ***$P < 0.001$

(Fig. 5B and Fig. S3) and THP-1 (Fig. 5C and Fig. S3) cells. These results indicated that the activity of NL101 was superior to that of vorinostat in synergizing with venetoclax in AML cells.

The combination of NL101 with venetoclax targets primary AML blasts ex vivo

To further validate the clinical utility of the NL101/venetoclax regimen, primary leukaemia cells were collected from 9 patients with de novo AML and 1 patient with relapsed AML, cultured, and treated with increasing
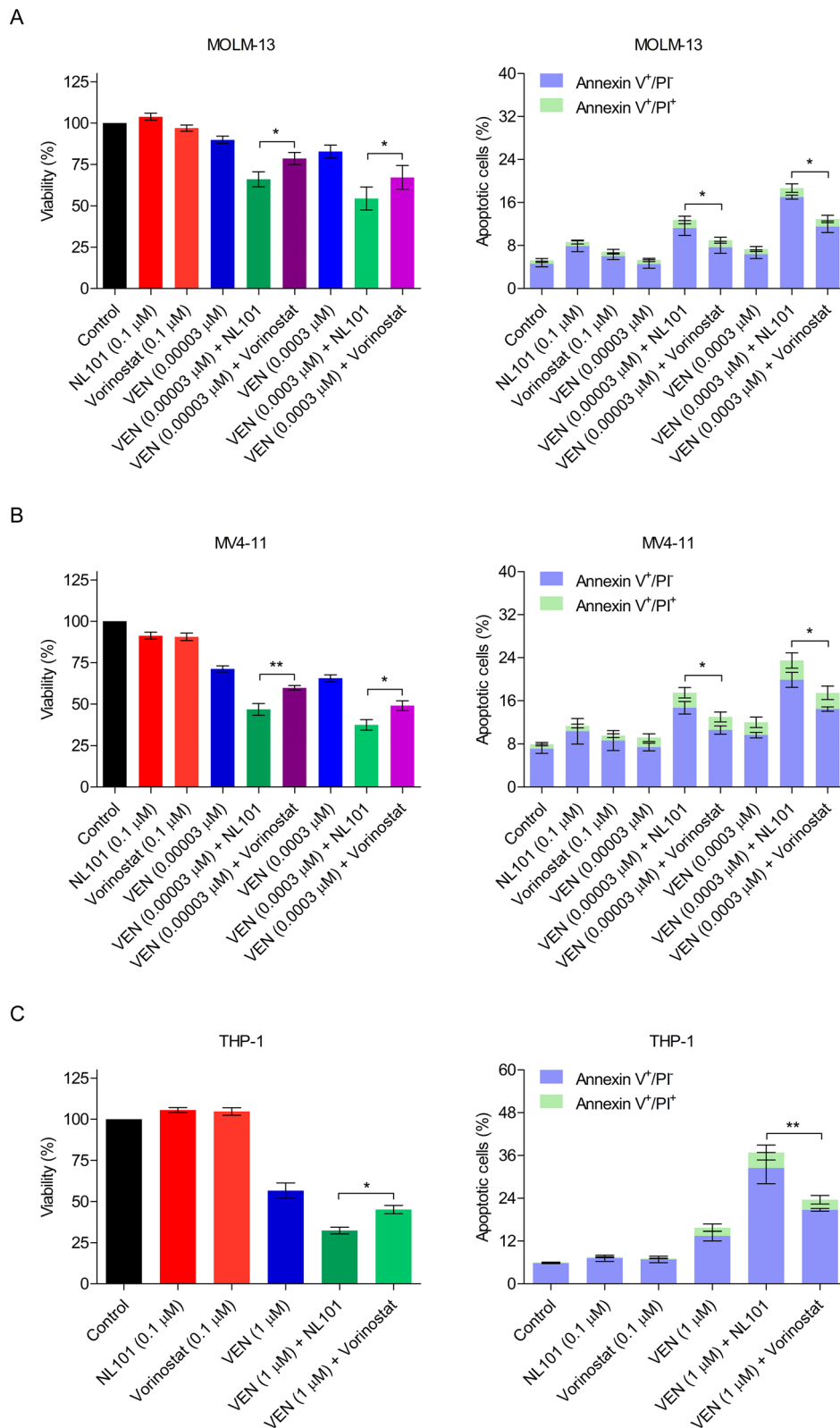
Fig. 5 Compared to vorinostat, NL101 shows superior synergistic activity with venetoclax in AML cells. MOLM-13 (**A**), MV4-11 (**B**), and THP-1 (**C**) cells were exposed to NL101, vorinostat, and venetoclax alone or in combination at the indicated concentrations for 48 h. Viability and apoptosis were then evaluated. *$P < 0.05$ and **$P < 0.01$

concentrations of NL101, venetoclax, or the combination ex vivo. The patients' characteristics were summarized in Table 1. The samples showed variable sensitivity to NL101 as a single agent, with IC_{50} values ranging from 0.86 to 4.14 μM after 24 h of treatment (Table 2). A cell viability assay revealed that all the tested patient samples responded to the combination of NL101 and venetoclax, and CI calculation as well as isobologram analysis demonstrated the presence of synergy between the two drugs across different AML subgroups (Fig. 6 and Fig. S4). Notably, sample #14 from the patient with relapsed AML was completely resistant to venetoclax and was highly insensitive to NL101. When combined, however, NL101 and venetoclax resulted in efficacy superior to that of either agent alone, as evidenced by the CI values of less than 0.52 for all combinations (Fig. 6). Although 1 μM NL101 alone did not significantly induce apoptosis in sample #5 (13.3% versus 8.4% in the control), it potently augmented venetoclax-induced apoptosis (Fig. 7A and Fig. S5). Similarly, synergistic induction of apoptosis was observed in samples #6, #17, #20, and #26 (Fig. 7A and Fig. S5). In agreement with these findings, cotreatment with 0.3 μM NL101 and 0.0001 μM venetoclax resulted in greater cleavage of PARP and caspase 3 than did either single-agent treatment, accompanied by increased downregulation of MCL-1 and BCL-xL, in samples #17 and #20 (Fig. 7B). Overall, these data suggested that NL101 and venetoclax exhibited synergistic effects against primary AML blasts, strengthening the clinical relevance of this combination.

Combined administration of NL101 and venetoclax prolongs animal survival in a murine AML model

Finally, to assess the activity and safety of the combination of NL101 and venetoclax in vivo, we established an AML xenograft model by inoculating NCG mice with

Table 2 Calculated IC_{50} for NL101 in primary AML samples

| Primary AML	IC_{50} at 24 h (μM) (95% CI)
#5	1.43 (0.98–2.08)
#8	3.06 (1.49–6.28)
#14	4.14 (1.29–13.35)
#17	3.45 (2.45–4.85)
#20	0.86 (0.65–1.13)
#21	2.28 (1.58–3.29)
#23	1.23 (0.98–1.53)
#24	1.72 (1.27–2.33)
#26	2.36 (1.58–3.52)

luciferase-labelled MV4-11 cells (denoted as Day 0). On Day 7, the mice were randomly assigned to one of four arms and treated with vehicle, venetoclax (75 mg/kg, QD×14, orally), NL101 (12 mg/kg, QD×2, intravenously), or the combination of venetoclax and NL101 (Fig. 8A). Bioluminescence imaging revealed that the bioluminescence signals indicating leukaemia prominently diminished over time in mice receiving NL101 plus venetoclax compared to those receiving either single drug (Fig. 8B), particularly on Day 14 (Fig. 8C). In agreement with these findings, alleviation of the leukaemia burden by the combined treatment was further verified by flow cytometric analyses of bone marrow samples obtained on Day 19, which revealed a marked reduction in the percentage of human $CD45^{+}$ cells (Fig. 8D). Most importantly, coadministration of NL101 and venetoclax effectively prolonged the survival of the animals, with significantly longer survival times in the combination treatment group than that in the groups treated with each drug alone (Fig. 8E; *P* values 0.0084 and 0.0091 for cotreatment versus venetoclax or NL101 alone, respectively). Notably, neither obvious weight loss nor other

Table 1 Patients' characteristics

Patient	Gender	Age (yr)	FAB	Blast purity (%)	Molecular mutations
#5	Male	51	M4	84	CBFB::MYH11, WT1, NRAS
#6	Male	55	M3	53	NA
#8	Male	30	M3	92	WT1, PML::RARA, FLT3
#14	Male	72	M5	63	FLT3-ITD, NRAS, RUNX1, SF3B1, BCOR
#17	Female	50	M5	93	WT1, FLT3
#20	Male	78	M2a	89	NA
#21	Male	53	M2a	84	BCR::ABL1, RUNX1
#23	Male	52	M2a	80	MECOM
#24	Female	59	M2a	60	WT1, FLT3, NRAS, DNMT3A
#26	Male	65	M2a	88	WT1, DNMT3A, FLT3, NPM1, TET2

Samples #5, #20, #23 and #26 were collected from peripheral blood. Samples #6, #8, #14, #17, #21 and #24 were collected from bone marrow

NA not available

Lu *et al. Journal of Translational Medicine*   (2024) 22:867

Page 12 of 18
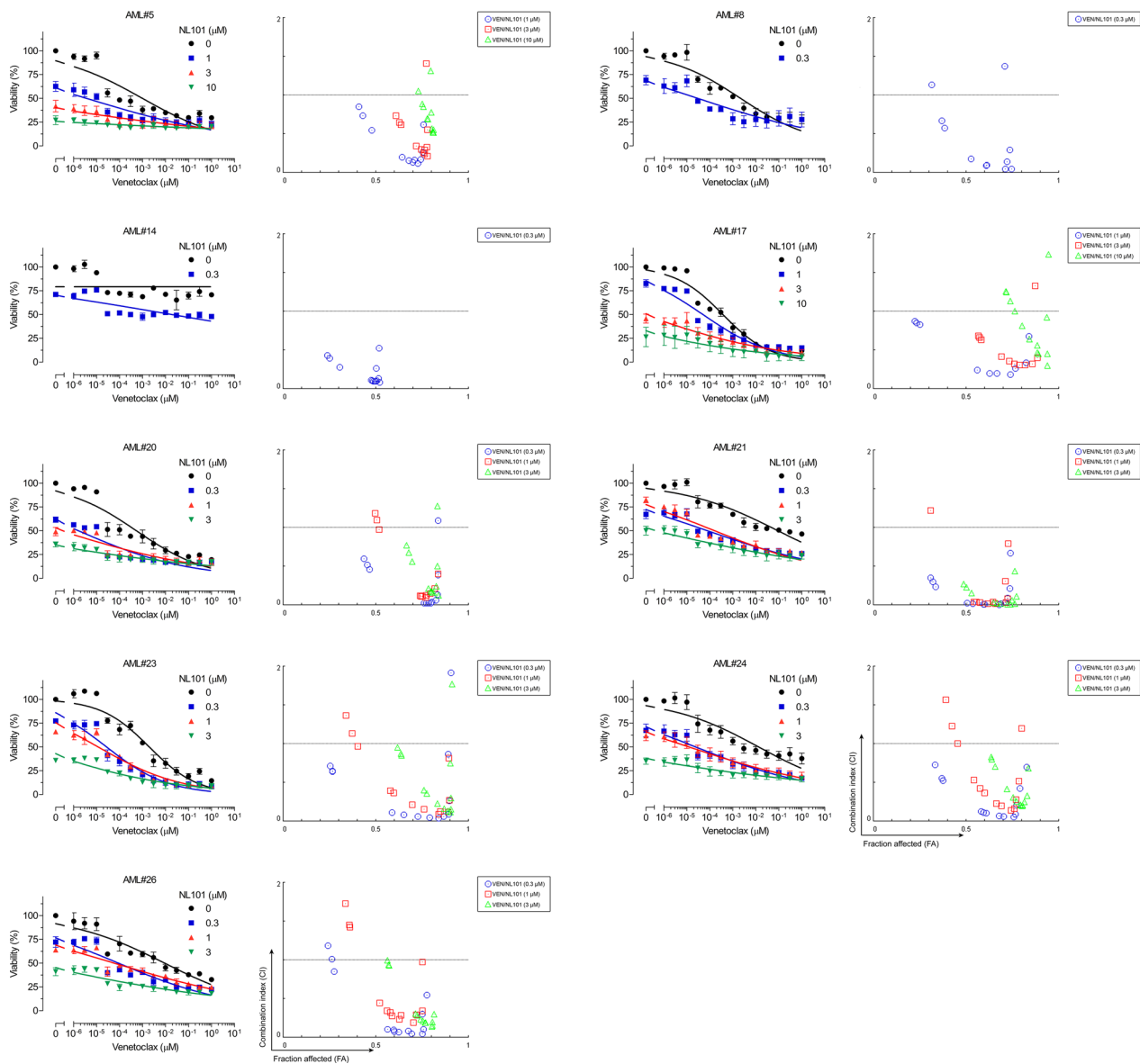
Fig. 6 NL101 combined with venetoclax synergistically reduces the viability in primary AML cells. Primary AML samples (#5, #8, #14, #17, #20, #21, #23, #24, and #26) were cotreated with NL101 and venetoclax at prespecified concentrations for 24 h, after which cell viability was measured and CI values were calculated
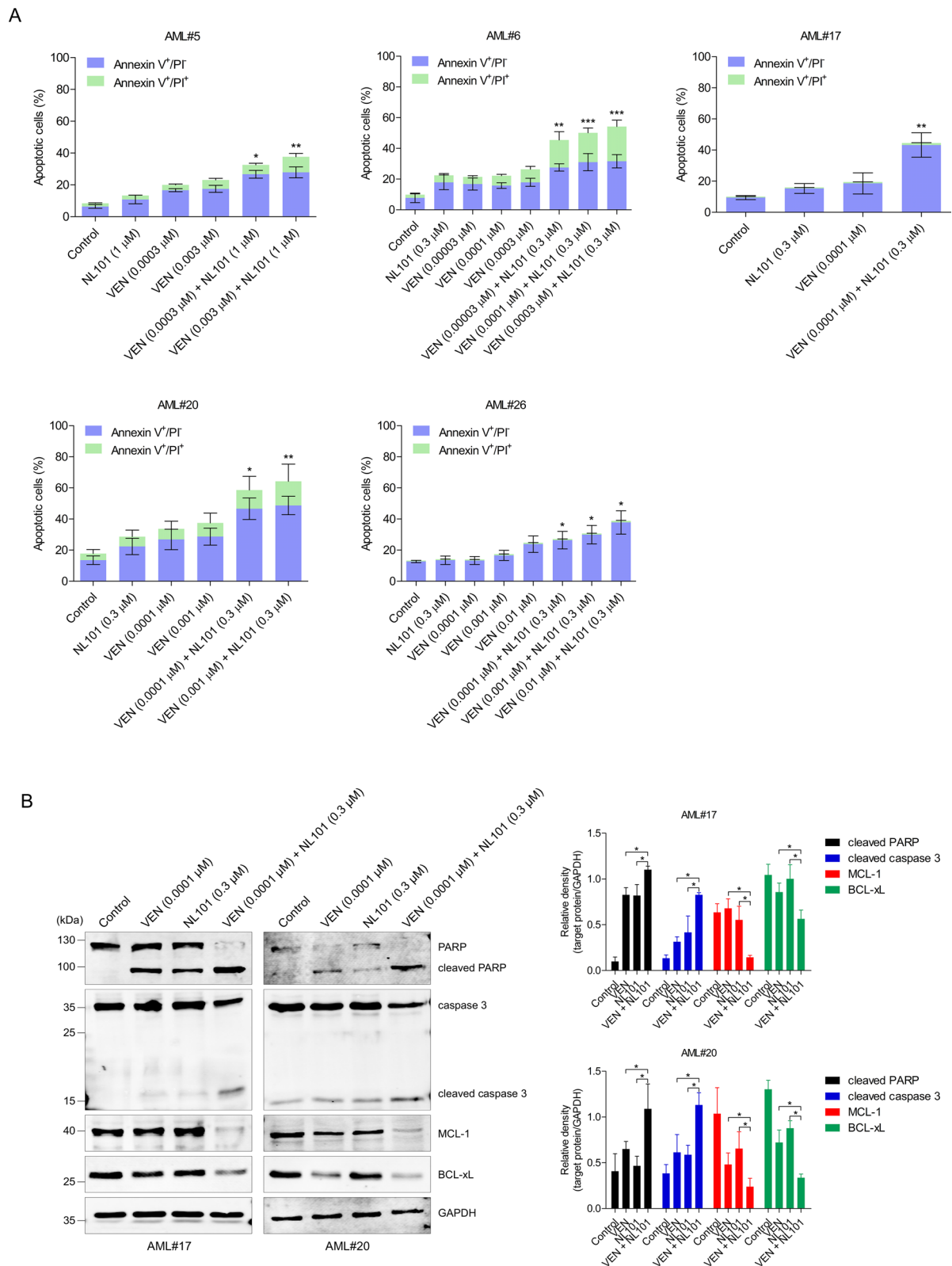
adverse events was observed throughout the treatment course, indicating that the NL101/venetoclax regimen was well tolerated (Fig. 8F). Therefore, these results demonstrated that NL101 can synergize with venetoclax in vivo.
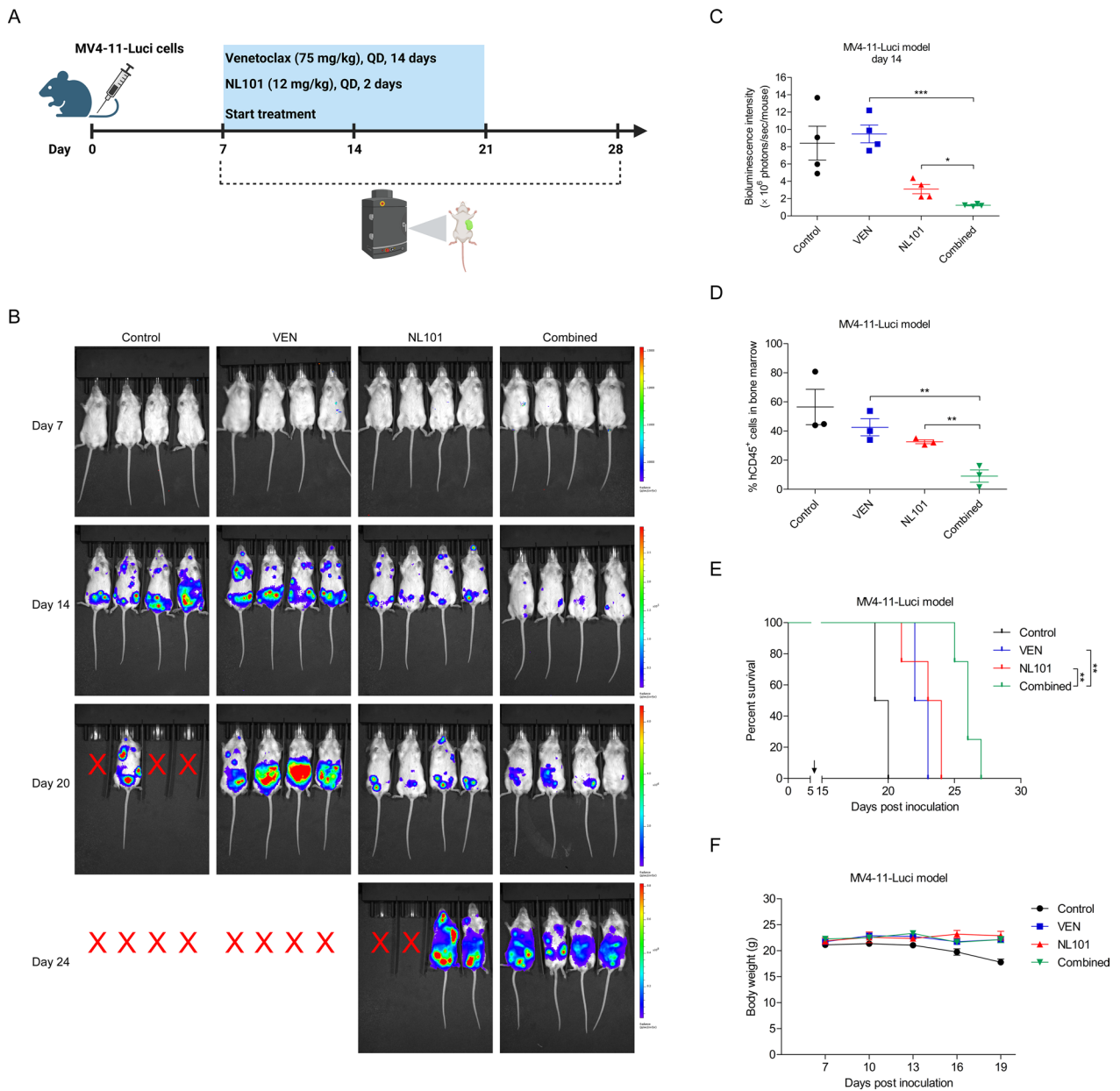
Discussion

The treatment paradigm for AML has been rapidly developing in the past few years since the recent approval of several new targeted inhibitors. In particular, the combination of the oral highly selective BCL-2 inhibitor

venetoclax with an HMA or LDAC has significantly improved outcomes in the population of older unfit patients, a previously difficult-to-manage population. These currently available less intensive regimens have tremendously altered the therapeutic landscape of AML and have prompted further investigations of additional venetoclax-based approaches, such as combinations with intensive chemotherapy and small molecule inhibitors. Preclinical data have shown synergy between venetoclax and both cytarabine and anthracycline drugs in AML cell lines and in primary AML samples [27, 28], providing

Fig. 7 NL101 combined with venetoclax synergistically induces apoptosis in primary AML cells. **A** Flow cytometry analysis of apoptosis in primary AML samples (#5, #6, #17, #20, and #26). *$P < 0.05$, **$P < 0.01$, and ***$P < 0.001$ versus the control group. **B** The protein levels of PARP (full-length and cleaved), caspase 3 (full-length and cleaved), MCL-1, and BCL-xL in primary AML samples (#17 and #20) measured via western blotting. GAPDH was used as a loading control. Representative blots from three independent experiments and densitometric analyses were shown. *$P < 0.05$

Fig. 8 In vivo administration of NL101 and venetoclax decreases the leukaemia burden and prolongs animal survival in an AML xenograft model. **A** Experimental scheme. Luciferase-expressing MV4-11 cells (1×10^7) were injected into NCG mice via the tail vein (Day 0), and treatment was initiated on Day 7. **B** AML progression was monitored through the IVIS imaging system. The red crossed lines indicated that the corresponding mice were euthanized upon the appearance of lower extremity paralysis. **C** Quantification of bioluminescence signals on Day 14. *$P < 0.05$ and ***$P < 0.001$. **D** Bone marrow was harvested from flushed tibias and femurs, and the percentage of human CD45+ cells was determined via flow cytometry. **$P < 0.01$. **E** Survival curves of the mice were generated via Kaplan–Meier analysis. The arrow indicated the time of treatment initiation (Day 7). **$P < 0.01$. **F** The body weights of the mice were monitored throughout the experiment

the rationale for a phase Ib trial (CAVEAT) that assesses the safety and efficacy of the combination of venetoclax with a modified "5 + 2" intensive chemotherapy regimen in older patients (aged 63–80 years) with newly diagnosed or secondary AML (sAML) without prior exposure to intensive chemotherapy [29]. This combination

treatment is tolerable and results in an overall response rate (ORR) of 72%. As expected, the ORR of patients with de novo AML (97%) is higher than that of patients with sAML (43%). Approximately 30% of adult AML patients carry FLT3 mutations (FLT3-ITD and FLT3-TKD), which result in an adverse prognosis [30], thus, FLT3 inhibition

Lu *et al. Journal of Translational Medicine*   (2024) 22:867

Page 15 of 18

is an attractive therapeutic strategy. As FDA-approved FLT3 inhibitors, midostaurin and gilteritinib synergistically enhance the effect of venetoclax through decreases in the protein levels of MCL-1 and p-ERK in models of FLT3-mutated AML [31]. Similarly, mutations in IDH1 or IDH2 have been identified in approximately 20% of AML patients [32], and it has been suggested that the FDA-approved IDH2 inhibitor enasidenib sensitizes IDH2-mutated AML to venetoclax [33]. Given these promising results, several ongoing clinical trials are now evaluating the combination of venetoclax with gilteritinib (NCT03625505) and quizartinib (NCT03735875) in patients with FLT3-mutated R/R AML, as well as with enasidenib (NCT04092179) in patients with IDH2-mutated myeloid malignancies. However, these mutation-specific inhibitors, administered as either monotherapies or as combination therapies with venetoclax, may not benefit the entire population of patients with AML. Drugs more extensively targeting leukaemogenesis are of great interest. To the best of our knowledge, we are the first to demonstrate the combined antileukaemic activity of NL101, a novel dual DNA/HDAC inhibitor, and venetoclax in preclinical AML models, laying the groundwork for the early phase of clinical investigation of this combination in patients.

A consensus has been reached, at least thus far, that venetoclax is unlikely to provide durable clinical benefit in patients with AML when administered as a single agent due to acquired resistance. Therefore, obtaining a deep understanding of the mechanisms underlying venetoclax resistance would be beneficial for developing proper venetoclax partners in order to maximize therapeutic efficacy in AML patients. The best characterized mechanism of resistance to venetoclax in AML is increased dependence on the alternative prosurvival proteins MCL-1 and BCL-xL. A shift towards upregulation of MCL-1/BCL-xL accompanied by downregulation of BCL-2 has been observed in venetoclax-resistant AML cell lines established by chronic venetoclax exposure [34]. Consequently, compensatory sequestration of venetoclax-freed BIM by MCL-1 prevents apoptosis [28]. This observation is confirmed by our results showing that the interaction between BIM and MCL-1 is markedly enhanced after venetoclax treatment. Venetoclax and the selective MCL-1 inhibitor VU661013, when used sequentially or simultaneously in combination, results in enhanced inhibitory effects compared with those of either agent alone both in AML cell lines and in patient-derived xenograft models [35]. Based on positive preclinical data, multiple novel MCL-1 inhibitors are in early stages of clinical development [36]. As NL101 is a SAHA-bendamustine hybrid, NL101-triggered apoptosis in AML cells is principally attributed to the dual effects

of HDAC inhibition (evidenced by hyperacetylation of histones and α-tubulin) and DNA damage (evidenced by the increase in γ-H2AX) [14] rather than to targeting of BCL-2 family proteins. Although the expression level of BCL-xL is reduced by NL101 in Kasumi-1 and NB4 cells [14], we could not reproduce this finding in MOLM-13 and THP-1 cells, probably due to the use of different cell lines and experimental conditions. In contrast, we found that MCL-1 and BCL-xL protein levels were elevated after NL101 treatment. However, the addition of NL101 to venetoclax led to simultaneous decreases in MCL-1 and BCL-xL levels in AML cells, which liberated the BH3-only activator protein BIM and ultimately activated apoptosis. Given the reliance of platelets on BCL-xL for survival and the lesson learned from navitoclax (ABT-263) [37, 38], we should always consider the theoretically possible toxicity of thrombocytopenia when this combination regimen is studied in humans. Thus, our work, along with that of other groups, confirms the importance of these prosurvival BCL-2 family proteins in supporting leukaemic blasts.

The transcription factor c-Myc is frequently dysregulated in AML, suggesting that this gene is an option for targeting [39, 40]. While direct inhibition of c-Myc has proven arduous, suppression of its expression and/or activity is feasible. Bromodomain and extraterminal (BET) proteins are known to drive the transcription and expression of c-Myc; thus, a class of BET inhibitors has been identified [41]. For example, mivebresib (ABBV-075) reduces c-Myc expression at both the transcriptional and translational levels and shows antileukaemic activity against cultured AML cell lines and patient-derived blast progenitor cells [42]. Moreover, mivebresib strongly enhances the efficacy of venetoclax in AML-engrafted immunodeficient mice, as well as in R/R AML patients [42, 43]. Similar results are obtained with 10058-F4, which inhibits c-Myc by disrupting the c-Myc/Max dimer [44]. These findings validate the key role of c-Myc in contributing to venetoclax resistance in AML. It has been suggested that SAHA acetylates c-Myc at lysine 323, resulting in c-Myc downregulation in AML cells [45]. As a SAHA-derived molecule, NL101 retains the ability to suppress c-Myc, even in the presence of venetoclax, suggesting an alternative approach for c-Myc targeting. The expression of c-Myc is regulated by multiple signal transduction pathways, including the PI3K/Akt and MEK/ERK pathways [46], which are also responsible for MCL-1 regulation. Akt and ERK have been shown to stabilize the MCL-1 protein via GSK3β and serum response factor/Elk-1, respectively [47, 48]. Thus, interruption of these cascades leads to the inhibition of c-Myc and/or MCL-1 and circumvents resistance to venetoclax. Via RNA-seq and immunoblotting, we discovered simultaneously
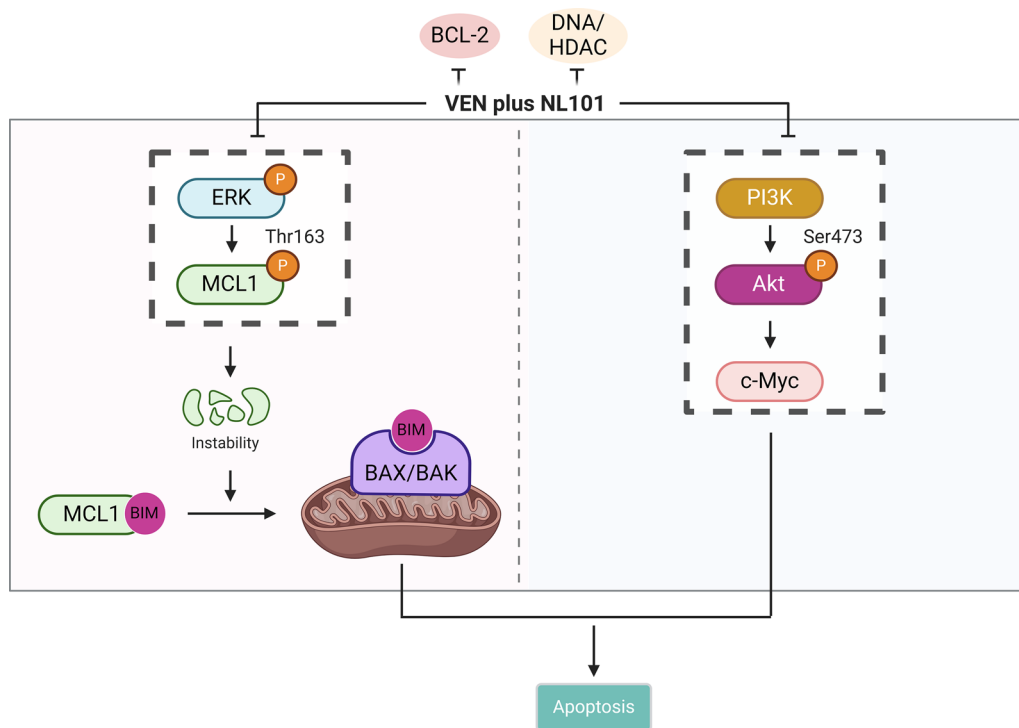
Fig. 9 Schematic illustration of the current study. The addition of NL101 to venetoclax decreases the stability of MCL-1 by inhibiting ERK, thereby facilitating the release of BIM and triggering mitochondrial apoptosis. Meanwhile, the strong synergy between NL101 and venetoclax also relies on the downregulation of c-Myc via PI3K/Akt/GSK3β signalling

decreased levels of phosphorylated Akt and ERK in AML cells treated with the combination of NL101 and venetoclax, at least partially revealing the mechanisms underlying the synergy between NL101 and venetoclax. In line with our observations, a recent study demonstrates that the HDAC/PI3K dual inhibitor CUDC-907 synergizes with venetoclax through downregulation of MCL-1 and c-Myc in preclinical models of AML [44].

In addition to its effect on c-Myc, we also found that NL101 alone or in combination with venetoclax strikingly reduced the expression level of another oncogenic transcription factor, c-Myb, in AML cells (data not shown), suggesting that c-Myb is a potential mediator of venetoclax resistance and that NL101 is a novel candidate for c-Myb targeting. Due to the requirement of c-Myb for normal bone marrow haematopoiesis in adults [49], additional studies are needed to elucidate the mechanism of NL101-induced c-Myb degradation and the influence of NL101 on the self-renewal and multilineage differentiation of haematopoietic stem cells.

Conclusions

In summary, we demonstrate the strong synergistic effect of NL101 in combination with venetoclax in AML cell lines, patient-derived primary blasts, and xenograft animal models. Simultaneous inhibition of MCL-1 and c-Myc through ERK and PI3K, respectively, is a potential mechanism (Fig. 9). These findings identify NL101 as a new agent for augmenting BCL-2 inhibition in AML therapy and support the pursuit of its clinical translation.

Abbreviations

AML	Acute myeloid leukaemia
FLT3	Fms-like tyrosine kinase 3
IDH	Isocitrate dehydrogenase
BCL-2	B-cell lymphoma-2
R/R	Relapsed or refractory
HMAs	Hypomethylating agents
LDAC	Low-dose cytarabine
HDACs	Histone deacetylases
SAHA	Suberoylanilide hydroxamic acid
MM	Multiple myeloma
MCL-1	Myeloid cell leukaemia-1
GSK3β	Glycogen synthase kinase-3β
FBS	Foetal bovine serum
CI	Combination index
FITC	Fluorescein isothiocyanate

Lu *et al. Journal of Translational Medicine*   (2024) 22:867

Page 17 of 18

PI   Propidium iodide
MMP   Mitochondrial membrane potential
KEGG   Kyoto Encyclopedia of Genes and Genomes
DEGs   Differentially expressed genes
FDA   Food and Drug Administration

Supplementary Information

The online version contains supplementary material available at https://doi.org/10.1186/s12967-024-05647-0.

Supplementary Material 1.

Availability of data and materials
All data generated or analysed during this study are included in this published article.

Declarations

Ethics approval and consent to participate
Bone marrow or peripheral blood samples were collected from AML patients under a protocol approved by the Human Ethics Committee of the Affiliated People's Hospital of Ningbo University after written informed consent was obtained from each patient in accordance with the Declaration of Helsinki.

Consent for publication
All authors have read and discussed the manuscript and have agreed to submit it for publication.

Competing interests
The authors declare no competing interests.

Author details
[1]Department of Hematology, The Affiliated People's Hospital of Ningbo University, Ningbo, China. [2]Department of Pathology, and Zhejiang Key Laboratory of Pathophysiology, School of Basic Medical Sciences, Health Science Center, Ningbo University, Ningbo 315211, China. [3]Institute of Hematology, Ningbo University, Ningbo, China. [4]Department of Hematology, The First Affiliated Hospital, Zhejiang University School of Medicine, Hangzhou, Zhejiang, China.

References

1. Lowenberg B, Ossenkoppele GJ, van Putten W, Schouten HC, Graux C, Ferrant A, et al. High-dose daunorubicin in older patients with acute myeloid leukemia. N Engl J Med. 2009;361:1235–48.
2. Kantarjian HM, Kadia TM, DiNardo CD, Welch MA, Ravandi F. Acute myeloid leukemia: treatment and research outlook for 2021 and the MD Anderson approach. Cancer. 2021;127:1186–1120.
3. Siegel RL, Miller KD, Jemal A. Cancer statistics, 2020. CA Cancer J Clin. 2020;70:7–30.
4. Jaramillo S, Schlenk RF. Update on current treatments for adult acute myeloid leukemia: to treat acute myeloid leukemia intensively or non-intensively? That is the question. Haematologica. 2023;108:342–52.
5. Roman Diaz JL, Vazquez Martinez M, Khimani F. New approaches for the treatment of AML beyond the 7+3 regimen: current concepts and new approaches. Cancers. 2024;16:677.
6. Konopleva M, Pollyea DA, Potluri J, Chyla B, Hogdal L, Busman T, et al. Efficacy and biological correlates of response in a phase II study of venetoclax monotherapy in patients with acute myelogenous leukemia. Cancer Discov. 2016;6:1106–17.
7. DiNardo CD, Pratz K, Pullarkat V, Jonas BA, Arellano M, Becker PS, et al. Venetoclax combined with decitabine or azacitidine in treatment-naive, elderly patients with acute myeloid leukemia. Blood. 2019;133:7–17.
8. DiNardo CD, Jonas BA, Pullarkat V, Thirman MJ, Garcia JS, Wei AH, et al. Azacitidine and venetoclax in previously untreated acute myeloid leukemia. N Engl J Med. 2020;383:617–29.
9. Wei AH, Strickland SA Jr, Hou JZ, Fiedler W, Lin TL, Walter RB, et al. Venetoclax combined with low-dose cytarabine for previously untreated patients with acute myeloid leukemia: results from a phase Ib/II study. J Clin Oncol. 2019;37:1277–84.
10. Wei AH, Montesinos P, Ivanov V, DiNardo CD, Novak J, Laribi K, et al. Venetoclax plus LDAC for newly diagnosed AML ineligible for intensive chemotherapy: a phase 3 randomized placebo-controlled trial. Blood. 2020;135:2137–45.
11. Chakraborty S, Park CY. Pathogenic mechanisms in acute myeloid leukemia. Curr Treat Options Oncol. 2022;23:1522–34.
12. Schaefer EW, Loaiza-Bonilla A, Juckett M, DiPersio JF, Roy V, Slack J, et al. A phase 2 study of vorinostat in acute myeloid leukemia. Haematologica. 2009;94:1375–82.
13. Cai B, Lyu H, Huang J, Wang S, Lee CK, Gao C, et al. Combination of bendamustine and entinostat synergistically inhibits proliferation of multiple myeloma cells via induction of apoptosis and DNA damage response. Cancer Lett. 2013;335:343–50.
14. Yu J, Qiu S, Ge Q, Wang Y, Wei H, Guo D, et al. A novel SAHA-bendamustine hybrid induces apoptosis of leukemia cells. Oncotarget. 2015;6:20121–31.
15. Lopez-Iglesias AA, Herrero AB, Chesi M, San-Segundo L, Gonzalez-Mendez L, Hernandez-Garcia S, et al. Preclinical anti-myeloma activity of EDO-S101, a new bendamustine-derived molecule with added HDACi activity, through potent DNA damage induction and impairment of DNA repair. J Hematol Oncol. 2017;10:127.
16. Li S, He X, Gan Y, Zhang J, Gao F, Lin L, et al. Targeting miR-21 with NL101 blocks c-Myc/Mxd1 loop and inhibits the growth of B cell lymphoma. Theranostics. 2021;11:3439–51.
17. Jin J, Li X, Guo W, Li F, Huang J, Huang X, et al. Novel SAHAbendamustine hybrid NL101 in combination with daunorubicin synergistically suppresses acute myeloid leukemia. Oncol Rep. 2020;44:273–82.
18. Jin J, Mao S, Li F, Li X, Huang X, Yu M, et al. A novel alkylating deacetylase inhibitor molecule EDO-S101 in combination with cytarabine synergistically enhances apoptosis of acute myeloid leukemia cells. Med Oncol. 2019;36:77.
19. Besse L, Kraus M, Besse A, Bader J, Silzle T, Mehrling T, et al. The first-in-class alkylating HDAC inhibitor EDO-S101 is highly synergistic with proteasome inhibition against multiple myeloma through activation of multiple pathways. Blood Cancer J. 2017;7: e589.
20. Li X, Li C, Jin J, Wang J, Huang J, Ma Z, et al. High PARP-1 expression predicts poor survival in acute myeloid leukemia and PARP-1 inhibitor and SAHA-bendamustine hybrid inhibitor combination treatment synergistically enhances anti-tumor effects. EBioMedicine. 2018;38:47–56.
21. Chou TC. Drug combination studies and their synergy quantification using the Chou–Talalay method. Cancer Res. 2010;70:440–6.

Lu *et al. Journal of Translational Medicine*   (2024) 22:867

Page 18 of 18

22. Zhao M, Jiang X, Fang J, Lin Y, Li Y, Pei R, et al. The kava chalcone flavokawain B exerts inhibitory activity and synergizes with BCL-2 inhibition in malignant B-cell lymphoma. Phytomedicine. 2023;120: 155074.
23. Li Y, Zhao M, Lin Y, Jiang X, Jin L, Ye P, et al. Licochalcone A induces mitochondria-dependent apoptosis and interacts with venetoclax in acute myeloid leukemia. Eur J Pharmacol. 2024;968: 176418.
24. Jiang X, Lin Y, Zhao M, Li Y, Ye P, Pei R, et al. Platycodin D induces apoptotic cell death through PI3K/AKT and MAPK/ERK pathways and synergizes with venetoclax in acute myeloid leukemia. Eur J Pharmacol. 2023;956: 175957.
25. Richon VM, Garcia-Vargas J, Hardwick JS. Development of vorinostat: current applications and future perspectives for cancer therapy. Cancer Lett. 2009;280:201–10.
26. Olsen EA, Kim YH, Kuzel TM, Pacheco TR, Foss FM, Parker S, et al. Phase IIb multicenter trial of vorinostat in patients with persistent, progressive, or treatment refractory cutaneous T-cell lymphoma. J Clin Oncol. 2007;25:3109–15.
27. Teh TC, Nguyen NY, Moujalled DM, Segal D, Pomilio G, Rijal S, et al. Enhancing venetoclax activity in acute myeloid leukemia by co-targeting MCL1. Leukemia. 2018;32:303–12.
28. Niu X, Zhao J, Ma J, Xie C, Edwards H, Wang G, et al. Binding of released Bim to Mcl-1 is a mechanism of intrinsic resistance to ABT-199 which can be overcome by combination with daunorubicin or cytarabine in AML cells. Clin Cancer Res. 2016;22:4440–51.
29. Chua CC, Roberts AW, Reynolds J, Fong CY, Ting SB, Salmon JM, et al. Chemotherapy and venetoclax in elderly acute myeloid leukemia trial (CAVEAT): a phase Ib dose-escalation study of venetoclax combined with modified intensive chemotherapy. J Clin Oncol. 2020;38:3506–17.
30. Levis M, Small D. FLT3: ITDoes matter in leukemia. Leukemia. 2003;17:1738–52.
31. Ma J, Zhao S, Qiao X, Knight T, Edwards H, Polin L, et al. Inhibition of Bcl-2 synergistically enhances the antileukemic activity of midostaurin and gilteritinib in preclinical models of FLT3-mutated acute myeloid leukemia. Clin Cancer Res. 2019;25:6815–26.
32. DiNardo CD, Ravandi F, Agresta S, Konopleva M, Takahashi K, Kadia T, et al. Characteristics, clinical outcome, and prognostic significance of IDH mutations in AML. Am J Hematol. 2015;90:732–6.
33. Cathelin S, Sharon D, Subedi A, Cojocari D, Phillips DC, Leverson JD, et al. Enasidenib-induced differentiation promotes sensitivity to venetoclax in IDH2-mutated acute myeloid leukemia. Leukemia. 2022;36:869–72.
34. Lin KH, Winter PS, Xie A, Roth C, Martz CA, Stein EM, et al. Targeting MCL-1/BCL-XL forestalls the acquisition of resistance to ABT-199 in acute myeloid leukemia. Sci Rep. 2016;6:27696.
35. Ramsey HE, Fischer MA, Lee T, Gorska AE, Arrate MP, Fuller L, et al. A novel MCL1 inhibitor combined with venetoclax rescues venetoclax-resistant acute myelogenous leukemia. Cancer Discov. 2018;8:1566–81.
36. Roberts AW, Wei AH, Huang DCS. BCL2 and MCL1 inhibitors for hematologic malignancies. Blood. 2021;138:1120–36.
37. Schoenwaelder SM, Jarman KE, Gardiner EE, Hua M, Qiao J, White MJ, et al. Bcl-xL-inhibitory BH3 mimetics can induce a transient thrombocytopathy that undermines the hemostatic function of platelets. Blood. 2011;118:1663–74.
38. Roberts AW, Seymour JF, Brown JR, Wierda WG, Kipps TJ, Khaw SL, et al. Substantial susceptibility of chronic lymphocytic leukemia to BCL2 inhibition: results of a phase I study of navitoclax in patients with relapsed or refractory disease. J Clin Oncol. 2012;30:488–96.
39. Baer MR, Augustinos P, Kinniburgh AJ. Defective c-myc and c-myb RNA turnover in acute myeloid leukemia cells. Blood. 1992;79:1319–26.
40. Takao S, Forbes L, Uni M, Cheng S, Pineda JMB, Tarumoto Y, et al. Convergent organization of aberrant MYB complex controls oncogenic gene expression in acute myeloid leukemia. Elife. 2021;10: e65905.
41. Stathis A, Bertoni F. BET proteins as targets for anticancer treatment. Cancer Discov. 2018;8:24–36.
42. Fiskus W, Cai T, DiNardo CD, Kornblau SM, Borthakur G, Kadia TM, et al. Superior efficacy of cotreatment with BET protein inhibitor and BCL2 or MCL1 inhibitor against AML blast progenitor cells. Blood Cancer J. 2019;9:4.
43. Borthakur G, Odenike O, Aldoss I, Rizzieri DA, Prebet T, Chen C, et al. A phase 1 study of the pan-bromodomain and extraterminal inhibitor mivebresib (ABBV-075) alone or in combination with venetoclax in patients with relapsed/refractory acute myeloid leukemia. Cancer. 2021;127:2943–53.
44. Li X, Su Y, Hege K, Madlambayan G, Edwards H, Knight T, et al. The HDAC and PI3K dual inhibitor CUDC-907 synergistically enhances the antileukemic activity of venetoclax in preclinical models of acute myeloid leukemia. Haematologica. 2021;106:1262–77.
45. Nebbioso A, Carafa V, Conte M, Tambaro FP, Abbondanza C, Martens J, et al. c-Myc modulation and acetylation is a key HDAC inhibitor target in cancer. Clin Cancer Res. 2017;23:2542–55.
46. Carter JL, Hege K, Yang J, Kalpage HA, Su Y, Edwards H, et al. Targeting multiple signaling pathways: the new approach to acute myeloid leukemia therapy. Signal Transduct Target Ther. 2020;5:288.
47. Townsend KJ, Zhou P, Qian L, Bieszczad CK, Lowrey CH, Yen A, et al. Regulation of MCL1 through a serum response factor/Elk-1-mediated mechanism links expression of a viability-promoting member of the BCL2 family to the induction of hematopoietic cell differentiation. J Biol Chem. 1999;274:1801–13.
48. Yoshimoto G, Miyamoto T, Jabbarzadeh-Tabrizi S, Iino T, Rocnik JL, Kikushige Y, et al. FLT3-ITD up-regulates MCL-1 to promote survival of stem cells in acute myeloid leukemia via FLT3-ITD-specific STAT5 activation. Blood. 2009;114:5034–43.
49. Lieu YK, Reddy EP. Conditional c-myb knockout in adult hematopoietic stem cells leads to loss of self-renewal due to impaired proliferation and accelerated differentiation. Proc Natl Acad Sci USA. 2009;106:21689–94.

Publisher's Note